

CityFlow-NL: Tracking and Retrieval of Vehicles at City Scale by Natural Language Descriptions

Qi Feng
Boston University
fung@bu.edu

Vitaly Ablavsky
University of Washington
vxa@uw.edu

Stan Sclaroff
Boston Univeristy
sclaroff@bu.edu

Abstract

Natural Language (NL) descriptions can be one of the most convenient or the only way to interact with systems built to understand and detect city scale traffic patterns and vehicle-related events. In this paper, we extend the widely adopted CityFlow Benchmark with NL descriptions for vehicle targets and introduce the CityFlow-NL Benchmark. The CityFlow-NL contains more than 5,000 unique and precise NL descriptions of vehicle targets, making it the first multi-target multi-camera tracking with NL descriptions dataset to our knowledge. Moreover, the dataset facilitates research at the intersection of multi-object tracking, retrieval by NL descriptions, and temporal localization of events. In this paper, we focus on two foundational tasks: the Vehicle Retrieval by NL task and the Vehicle Tracking by NL task, which take advantage of the proposed CityFlow-NL benchmark and provide a strong basis for future research on the multi-target multi-camera tracking by NL description task.

1. Introduction

Understanding city-wide traffic patterns and detecting specific vehicle-related events in real time has applications ranging from urban planning and traffic-engineering to law enforcement. In such applications, Natural Language (NL) descriptions can be one of the most convenient or the only way to interact with a computer system, *e.g.* taking as input an informal description provided by a bystander. Thus, it becomes necessary to detect, track and retrieve vehicles, potentially seen from multiple spatio-temporally disjoint viewpoints, based on NL queries.

Motivated by this demand, we define and address the task of Multi-Target Multi-Camera (MTMC) by NL Description. The goal of this task is to track a specific target described by an NL query within a sequence of multi-view video in the form of a sequence of bounding boxes on each camera view. While it shares similarities with

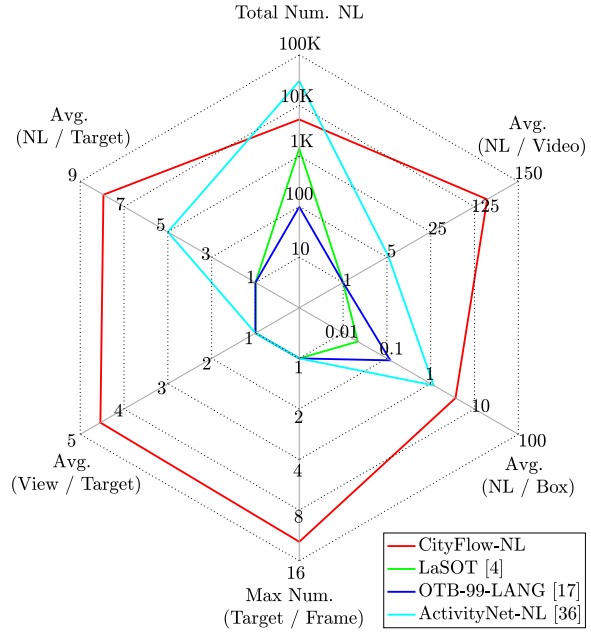


Figure 1: Comparison between NL annotated visual tracking datasets. The proposed CityFlow-NL is the first natural language multi-view multi-target tracking benchmark.

other Vision+NL tasks like single object tracking (potentially without distraction) by NL [5, 6, 17], NL-based video retrieval [1, 39], and spatio-temporal localization by NL [7, 13, 36], the proposed task requires both temporal and spatial localization of the target from a multi-view video via an NL query. Up until now, an added challenge in developing and evaluating algorithms for the proposed task is the lack of realistic datasets.

Therefore, we introduce CityFlow-NL, an open dataset designed to facilitate research at the intersection of multi-object tracking, retrieval by NL specification, and temporal localization of events. Our benchmark is derived from CityFlow [31], which is itself a public dataset that has been at the center of several recent workshop-challenges focused on MTMC tracking and re-identification [22, 23, 24, 25].

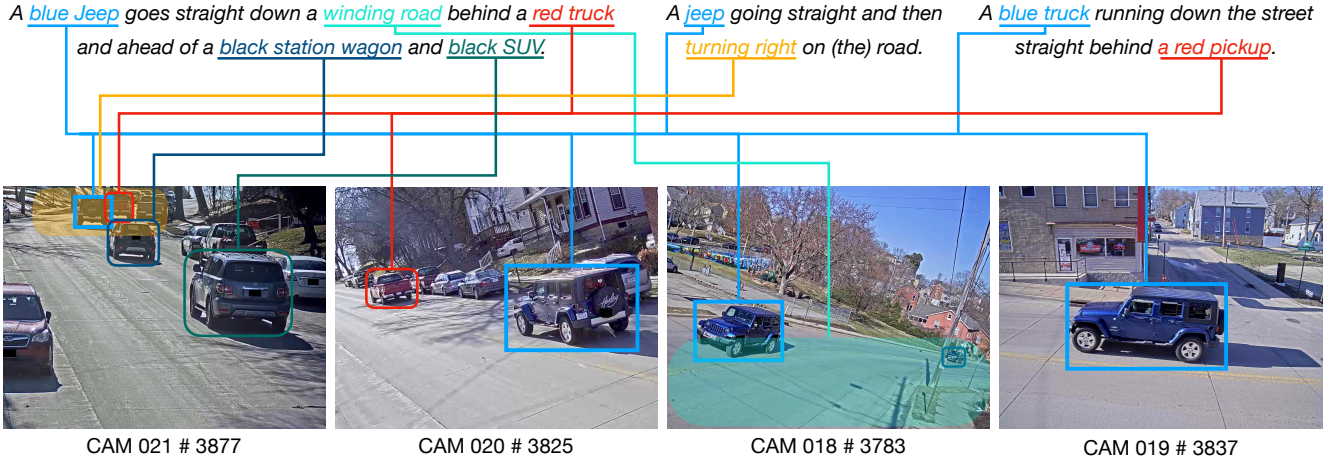


Figure 2: Example frames and NL descriptions from the proposed CityFlow-NL dataset. Crowdsourcing workers annotate the target vehicle using a carefully designed multi-camera annotation platform (Fig. 4). NL descriptions we collect tend to describe vehicle color/type (e.g. *blue Jeep*), vehicle motion (e.g. *turning right* and *straight*), traffic scene (e.g. *winding road*), and relations with other vehicles (e.g. *red truck*, *black SUV*, etc.).

As a result, the proposed CityFlow-NL dataset exhibits a diversity of real-world parameters, including traffic density and patterns, viewpoints, ambient conditions, etc.

The NL descriptions are provided by at least three crowdsourcing workers, thus capturing realistic variations and ambiguities that one could expect in such application domains. Crowdsourcing workers describe the target vehicle using a carefully designed multi-view annotation platform. The NL descriptions tend to describe the vehicle color, the vehicle maneuver, the traffic scene, and relations with other vehicles. Example NL descriptions and vehicle targets are shown in Fig. 2.

Although the motivation for building the CityFlow-NL dataset is to tackle the real-world problem of MTMC by NL, the introduction of the CityFlow-NL also opens up research possibilities for the retrieval/tracking by NL tasks to more advanced topics, e.g. action recognition by NL and spatio-temporal relation understanding problems. In this paper, we propose two basic tasks: the vehicle retrieval by NL description task and the vehicle tracking by NL description task. We consider these tasks as a foundation for more advanced Vision+NL tasks, including the MTMC by NL task.

Given a sequence of a *single-view* video and an NL description that uniquely describes a vehicle target in the video, the goal of the vehicle tracking task is to predict a spatio-temporal localization in the form of a sequence of bounding boxes for the target. The vehicle retrieval task is a simpler form of the tracking task, in which the spatial localizations of all candidate vehicles are given and the goal is to retrieve the target specified by the NL query. These tasks are related to object tracking and retrieval systems and can be evaluated in a similar way, but the NL query setup poses unique challenges. For example, relationship expressions

between targets (Fig. 2) and spatial referring expressions (Fig. 11) have not been investigated in visual trackers.

2. Related Works

In the past decade, researchers have started to look into exploiting natural language understanding in computer vision tasks. These models usually consist of two components: a language model and an appearance model to learn a new feature space that is shared between both NL and visual appearance [15, 33]. More recent object detection and vision grounding models [11, 37] jointly exploit vision and NL using Siamese networks and depth-wise convolutional neural networks.

The VisualGenome [16], Flickr-30K [38] and Flickr-30K entities [26] benchmarks facilitate research in understanding language grounded in visual contents. These image datasets provide detailed descriptions of regions in an image but still lack temporal information that can enable systems to better handle the temporal context and motion patterns in the NL descriptions.

OTB-99-LANG [17] is the first open dataset that provides NL descriptions for single object tracking, followed by LaSOT [4] which is a large scale single object tracking benchmark annotated with NL descriptions. These datasets enable researchers to perform spatial localization of targets based on NL descriptions of the target objects. However, both of these datasets are annotated with one NL description for the target object for the entire sequence. The NL descriptions in OTB-99-LANG and LaSOT is limited to a sentence or a phrase during annotation and can be ambiguous when used for tracking. These NL descriptions are not able to describe the motion pattern of the target [5], espe-

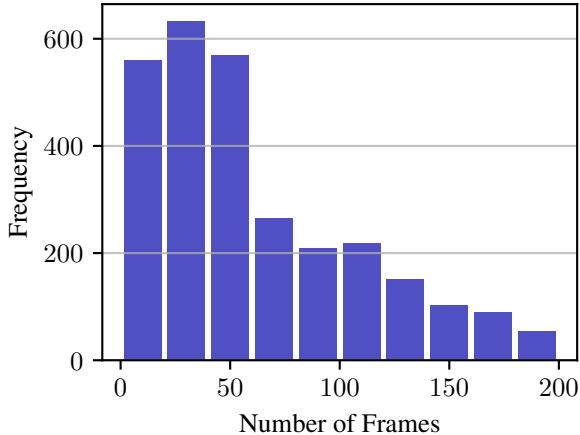


Figure 3: Histogram of number of frames vehicle targets shows in camera. The average number of frames is 75.85 frames, during which a vehicle target typically conducts a single maneuver and can be precisely described by an NL description in one sentence. Targets in existing single object tracking with NL benchmarks, *e.g.* OTB-99-LANG [17] and LaSOT [4], are not or cannot be precisely described by a sentence due to the length of the videos in these datasets.

cially over a longer time interval.

On the other hand, temporal localization of targets in videos using NL descriptions has gained research interest with the introduction of the DiDeMo dataset [1]. The DiDeMo dataset provides open domain videos with NL descriptions for temporal moment. Each NL description refers to a specific temporal moment and describes the main event in the video. However, DiDeMo does not provide spatial localization of the target within a frame and videos collected are intended for event recognition instead of tracking.

The spatial-temporal localization by NL description task is first introduced by Yamaguchi *et al.* [36]. The ActivityNet dataset is annotated with NL descriptions to facilitate the training and evaluation of the proposed task. However, the temporal retrieval in [36] entails retrieving the target video clip from a set of video clips. On the contrary, the goal of the proposed vehicle tracking and retrieval task is to temporally localize the target object within one sequence of video. Additionally, the targets in the ActivityNet-NL take up most of the frame and cannot serve as a tracking benchmark. In this paper, we focus on building a multi-target tracking with NL description benchmark. The NL descriptions can be used to localize targets both temporally and spatially in multi-view videos, providing benchmarks for multiple Vision+NL tasks.

3. CityFlow-NL Benchmark

In this section, we describe the statistics of the proposed CityFlow-NL benchmark and how we extend and annotate

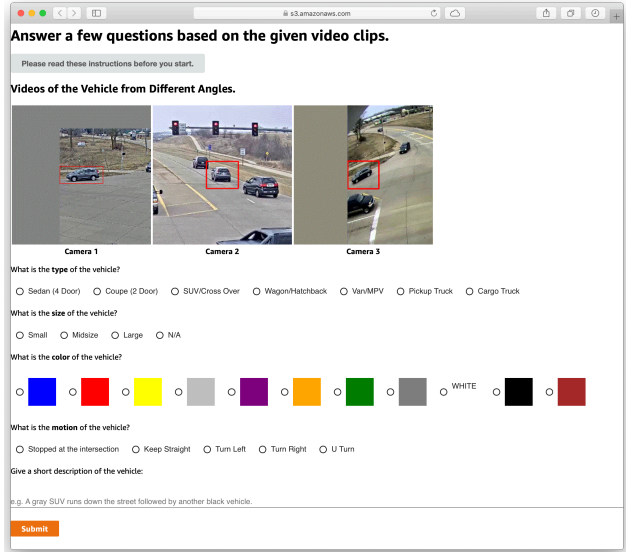


Figure 4: Screenshot of the platform we use to collect the CityFlow-NL dataset. Annotators are given detailed instructions on how to annotate NL descriptions for the vehicle targets presented in multi-view GIFs.

the CityFlow Benchmark [31].

3.1. Overview

We extend the CityFlow Benchmark with Natural Language (NL) Descriptions for each target vehicle. The CityFlow-NL makes it possible to build and evaluate systems that can jointly leverage both language and visual modalities. The proposed CityFlow-NL consists of 666 targets vehicles in 3,028 (single-view) tracks from 40 calibrated cameras, and 5,289 unique NL descriptions. The average number of frames a target vehicle shows in the CityFlow Benchmark is 75.85. The distribution of the number of frames of target vehicles is shown in Fig. 3.

A web based platform, shown in Fig. 4, is designed to collect NL annotations. We provide multi-view video clips with red bounding boxes drawn around each vehicle target and direct crowd-sourcing workers to give a detailed NL description of the target vehicle that can be used to uniquely identify the target vehicle from other vehicles. We collect annotations for each multi-view track with at least three crowd-sourcing workers from Amazon SageMaker.

We split multi-view tracks from the CityFlow Benchmark by the timestamps of cameras into multiple multi-view (or single-view) tracks that do not overlap with each other temporally. For example, if a target shows up in camera 1 and camera 2 in two temporal segments that do not overlap with each other, we generate two separate tracks for our annotation process. For each multi-view track, we clip video segments from all views with bounding boxes drawn

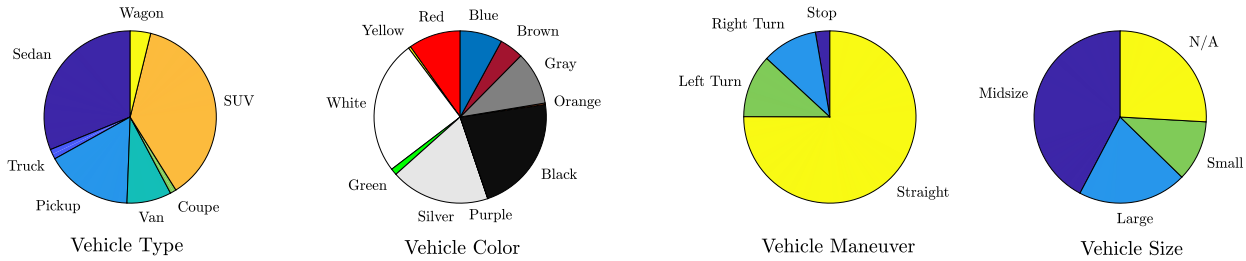


Figure 5: Distribution of vehicle type, color, maneuver, and size for the CityFlow-NL. A majority vote mechanism between three different annotators is implemented during the annotation process to automate the verification of the annotation and ensures the consensus and quality of the NL descriptions.

Dataset	# NL	T	MV	MT
CityFlow-NL	5,289	Yes	Yes	Yes
LaSOT [4]	1,400	Yes	No	No
OTB-99-LANG [17]	99	Yes	No	No
ActivityNet-NL [36]	30,365	No	No	No

Table 1: Comparison between NL annotated computer vision datasets. T stands for whether the dataset is designed for visual tracking; MV stands for multi-view (calibrated); MT stands for multi-target. The CityFlow-NL is the first MTMC for NL dataset and is the largest NL annotated tracking benchmark in terms of the number of NL.

around the target vehicle.

3.2. Collecting Attributes of Target Vehicle

Prior to a crowdsourcing worker generating an NL description (in the form of a declarative sentence of an arbitrary length), the crowdsourcing worker is asked to tag the multi-view video clip using predefined attributes. The distribution of these attributes are summarized in Fig. 5.

Performing such a preliminary task provides two benefits. First, it tends to focus every crowdsourcing worker’s attention on a common set of visual and linguistic concepts while crowdsourcing worker remain free to create an NL description in any form. Second, the attributes selected by crowdsourcing workers facilitate automatic verification of an crowdsourcing worker’s engagement with the task and consistency among the various crowdsourcing workers of the same video clip. Since we direct crowdsourcing workers to annotate NL descriptions in free form, it introduces uncertainty to the annotation process and a direct verification of the annotated NL descriptions is infeasible. Thus, a majority voting mechanism between annotations for the attributes (color, motion, maneuver) from three different crowdsourcing workers is used to automate the verification of the annotation and ensures the quality of the NL descriptions. If no agreement between the three workers is reached, the annotations are discarded and the target vehicle is re-annotated by another three workers.

As was the case with the CityFlow dataset [31], the per-

target attributes are not considered part of our CityFlow-NL dataset. One reason is that the designers of the CityFlow Benchmark made a decision to hide attributes when releasing their challenge dataset for the AI City Challenge [22], in part to prevent challenge participants from gaining unfair advantage. Another reason is that while attribute-based tracking received attention in the past [32], the motivation for using attributes is not as apparent given strong NL models, and the requirements of real-world scenarios. Indeed, as shown in [5] NL-based tracking decisively outperforms attribute-based tracking on a challenging benchmark. The attributes are not equivalent to the NL descriptions, where additional information including vehicle maneuver and relations to other targets are essential to a variety of problems.

3.3. Collecting NL Descriptions

NL descriptions of the same target can be very different, as NL descriptions are subjective and may focus on different aspects of the target. Examples of such annotations are shown in Fig. 2. The NL descriptions we collect tend to describe the vehicle color, the vehicle maneuver, the traffic scene, and the relation of the vehicle with other vehicles in the scene. We specifically direct crowdsourcing workers to describe the intrinsic motion for all maneuvers in the multi-view video clip. Moreover, some conflicting descriptions are acceptable due to color distortions and view-angle differences in these multi-view videos. Our majority vote mechanism identifies consensus among annotators, given the natural variation in their NL descriptions.

3.4. Comparison to Other NL+Vision Datasets

We compare the CityFlow-NL to other NL annotated vision datasets and presented in Fig. 1 and Tbl. 1. The CityFlow-NL is the first dataset built for the MTMC by NL task. Comparing to prior NL annotated video datasets, the proposed CityFlow-NL focuses on building a dataset for multi-object tracking and keeps the unique challenges for visual tracking as we discussed in Sec. 2. Each of the NL descriptions in our dataset describes a specific target for the entire duration in the multi-view video. Our annotation

process avoids potential observation and annotation biases from crowdsourcing workers for vehicle motion by presenting multi-view GIFs, using multiple-choice questions for attributes and a majority vote mechanism implemented during the annotation process.

4. Vehicle Retrieval by NL Task

We now define the Vehicle Retrieval by Natural Language Description Task and present how we use the proposed CityFlow-NL Benchmark for it. We consider this task as an essential first step towards tackling more advanced Vision+NL tasks like the MTMC by NL description task.

4.1. Task Definition

For the purpose of the retrieval by NL task, we utilize the proposed CityFlow-NL Benchmark in a *single-view* setup, although the CityFlow-NL could be used for retrieval tasks with multi-view tracks. For each single-view vehicle track, we bundle it with a query that consists of three different NL descriptions for training. During testing, the goal is to retrieve and rank vehicles tracks based on NL queries.

This variation of the proposed CityFlow-NL contains 2,498 tracks of vehicles with three unique NL descriptions each. Additionally, 530 unique vehicle tracks together with 530 query sets (each annotated with three NL descriptions) are curated for testing.

The proposed NL tracked-object retrieval task offers unique challenges versus action recognition tasks and content-based image retrieval tasks. In particular, different from prior content-based image retrieval systems [8, 14, 21], retrieval models for this task need to consider the relation contexts of a vehicle track and motion within the track as well. While the action recognition by NL description task [1] temporally localizes a moment within a video, the proposed tracked-object retrieval task requires both temporal and spatial localization within a video.

4.2. Evaluation Metrics

The Vehicle Retrieval by NL Description task is evaluated using standard metrics for retrieval tasks [20]. We use the Mean Reciprocal Rank (MRR) as the main evaluation metric. Recall @ 5, Recall @ 10, and Recall @ 25 are also evaluated for all models.

For each query in the testing split, we rank all 530 candidate tracks using the retrieval system and evaluate the retrieval performance based on the above-mentioned metrics.

4.3. The Retrieval Baseline Model

We build the baseline model to measure the similarities between a vehicle track \mathcal{T} and a NL description Q . Our baseline formulation is inspired by content-based image retrieval systems [38] and image captioning models [15, 33]. The overview of the baseline model is shown in Fig. 6.

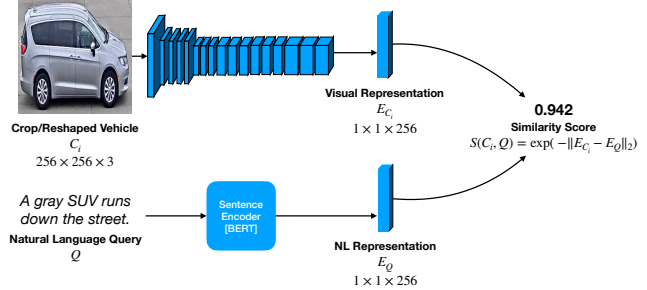


Figure 6: The baseline retrieval model inspired by content-based image retrieval models [8, 14, 21]. A similarity between the NL representation of the NL query and the visual representation of the input frame crop is measured by the Siamese network.

The vehicle track is defined as a sequence of frames in a video clip. $\mathcal{T} = \{F_1, \dots, F_t\}$. We use the ground truth bounding box of the target vehicle to crop each frame and reshape the sequence of crops, denoted as C , to the same shape of (256, 256). This sequence of reshaped frame crops of the target, $\{C_1, \dots, C_t\}$, is used as the visual representation of the vehicle. We build a Siamese embedding model for the retrieval task, where each crop C_i is embedded by a ResNet-50 [10] pretrained on ImageNet [29], denoted as E_{C_i} . We use a pretrained BERT [3] to embed the NL description Q into a 256 dimensional vector, denoted as E_Q .

The similarity between C_i and Q is defined as:

$$S(C_i, Q) = \exp(-\|E_{C_i} - E_Q\|_2). \quad (1)$$

For the baseline retrieval model, both positive and negative pairs of vehicle image crop C_i and Q are constructed for training. Negative pairs of C_i and Q are built by randomly selecting NL descriptions that describe other targets. The baseline retrieval model is trained with a cross entropy loss and an initial learning rate of 0.001 for 20 epochs on 2 GPUs using a stochastic gradient descent optimizer.

For the purpose of inference, we measure the similarity between a test track and a test query as the average of the similarities between all pairs of crops in the track and NL description in the test query. *i.e.*

$$S(\mathcal{T}, \{Q_1, Q_2, Q_3\}) = \frac{1}{3 \cdot t} \sum_{j=1}^3 \sum_{i=1}^t S(C_i, Q_j). \quad (2)$$

4.4. Retrieval Results and Analysis

For each test query, we compute this similarity on all test tracks and rank the tracks for evaluation. The baseline model achieves an MRR of 0.0269, Recall @ 5 of 0.0264, Recall @ 10 of 0.0491, Recall @ 25 of 0.1113.

An example of a failure case from the baseline retrieval model is shown in Fig. 7. In this specific case, positional referring expressions (“in the right lane”) is given in the NL



(a) A target vehicle track for retrieval. The NL descriptions given are: “A red wagon goes straight”, “Red SUV going straight in the right lane.” and “A red SUV head straight down the road.” The baseline retrieval model gives this track the average similarity score at 0.81 and ranks this track the fifth. Notice that the second NL description specified that the target is moving in the right lane.



(b) The baseline retrieval model ranks this track the first with the highest average similarity score at 0.84. This vehicle shares the same size, type, color, and motion pattern with the target vehicle for retrieval. The baseline retrieval model fails to capture the spatial referring expression (“in the right lane”) from the second NL description.

Figure 7: Example of a failed retrieval by the baseline retrieval model.

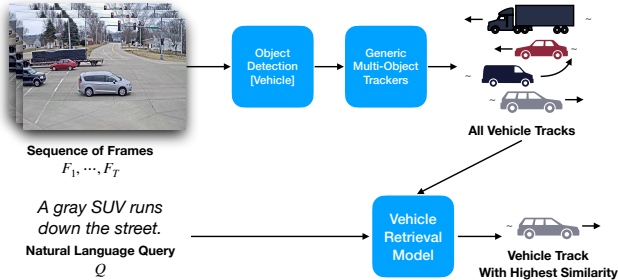


Figure 8: The baseline tracking model comprises three steps. The first step is to detect all vehicles in every frame. The second step is to utilize a generic multi-object tracker to obtain all vehicle tracks. In the last step, the baseline retrieval model is used to rank predicted tracks by their similarities and predict the target vehicle track.

description, but the baseline retrieval model does not consider the position of the target within the frame. Moreover, it is worth noting that the baseline model does not consider the motion pattern nor the context of vehicle tracks explicitly and the retrieval performance could be further improved by measuring the motion within the frame.

5. Vehicle Tracking by NL Task

We now describe how we use the proposed CityFlow-NL Benchmark for the vehicle tracking by NL description task.

5.1. Problem Definition

We further investigate the potential of the proposed retrieval model and extend it to the tracking by NL task. With the same query as in the retrieval task, together with a sequence of frames (F_1, \dots, F_T) as inputs, the goal is to

track the specific target the NL query refers to in the form of a sequence of bounding boxes. For each frame, the tracker should either predict the bounding box for the target or predict that the target is not present in the frame.

5.2. Evaluation Metrics

The vehicle tracking by NL description task is evaluated, following popular object tracking protocols, using the Area Under Curve (AUC) of the Success Rate vs. Intersection over Union (IoU) thresholds and Normalized Precision [35].

The success is defined as 0 for frames where the prediction is “not present” while the ground truth is available, or the ground truth is “not present” and a prediction is made. For frames with both a ground truth bounding box and a prediction, the success is measured by computing the IoU between the ground truth bounding box and the prediction and comparing this against a predefined threshold. The AUC of the success rate at different IoU thresholds is reported as the performance for each tracker [35].

5.3. The Tracking Baseline Model

Intuitively, to perform tracking of the target vehicle using NL descriptions, we use our baseline retrieval model introduced in Sec. 4.3 for inference on tracks predicted by multi-object trackers. The baseline model is shown in Fig. 8.

The tracking baseline model consists of three stages. The first stage of the model is an object detector which localizes all vehicles in every frame. In the second stage, we use a generic multi-object tracker to predict vehicle tracks on the test split of the CityFlow-NL. In the last stage, we use the baseline retrieval model introduced in Sec. 4.3 to rank the predicted vehicle tracks for each query. The vehicle track with the highest average similarity score is returned by the baseline tracker as the prediction.

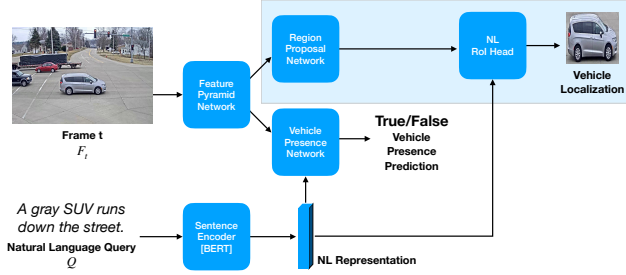


Figure 9: The proposed Vehicle Tracking Network (VTN) has two branches: an NL based Vehicle Presence branch and a NL based vehicle localization branch. The vehicle presence branch predicts whether the vehicle target of the given NL query is present in the given frame. The vehicle localization branch makes region proposals and predicts bounding boxes based on the NL query.

The baseline vehicle tracking model first localizes and tracks all vehicles in a video and predicts a retrieval score for each vehicle track in the second pass. The time complexity of retrieval baselines model is $O(M \times N)$, where M is the size of the query set and N is the number of tracks predicted by the multi-object tracker.

In our experiments, we tested our baseline tracker with three different multi-object trackers: DeepSORT [34], MOANA [30], and TNT [12] with three different sets of vehicle detections: MaskRCNN [9], YOLO3 [27], and SSD512 [19]. We use the same model we trained for the retrieval task for the tracking task. Results are summarized in Tbl. 2. Trackers using SSD detections are outperforming others with a higher recall rate. These baseline trackers are competitive with each other.

5.4. Vehicle Tracking Network (VTN)

Instead of the two-stage multi-object tracking and NL retrieval approach, we now introduce a more efficient and accurate Vehicle Tracking Network (VTN), which is summarized in Fig. 9. Similar to prior works on single object tracking with NL description [5, 6, 17], we design the VTN to be a one-shot tracker by detection that is adapted to utilize an NL description. The VTN first extracts the visual features of a frames F_t using a Feature Pyramid Network (FPN) [18]. The visual features are then used in two separate branches: a Vehicle Presence Network (VPN) and a Vehicle Localization Network (VLN).

The VPN, shown in Fig. 10, indicates the target’s presence in the given frame to initiate or terminate a track. The vehicle tracking by NL description task differs from single object tracking by NL description task [17] as the presence of the target is not guaranteed for most of the frames. Thus, a cross-correlation (XCorr) operation [2] between the NL representation and the visual features from the four stages of the FPN (“P2” thru “P5”) is used to localize the target

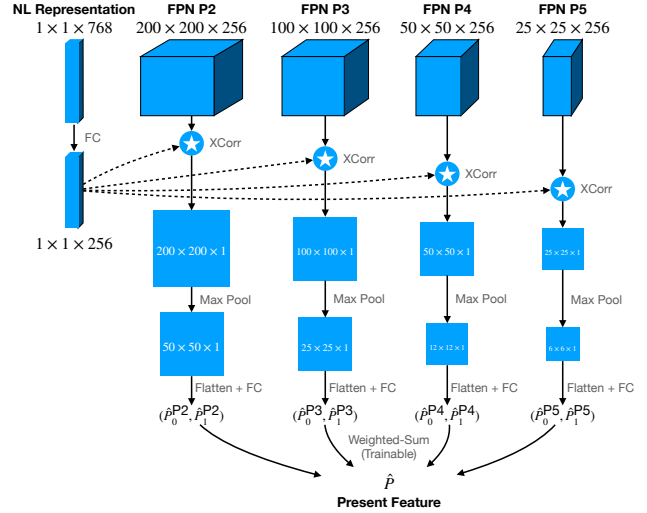


Figure 10: The Vehicle Presence Network (VPN), part of the proposed VTN, as shown in Fig. 9.

temporally. A weighted average trained between the four presence features is then used to compute the output presence feature, denoted as P . A softmax function between the two elements in P is used to determine the presence probability \hat{P} of the vehicle target based on the NL query, *i.e.*

$$\hat{P} = \frac{e^{P_1}}{e^{P_0} + e^{P_1}}. \quad (3)$$

We use P^* to denote the ground truth presence of the target, where $P^* = 1$ represents the presence and $P^* = 0$ represents that the target is not present in the frame. A binary cross entropy loss is used to train the presence branch:

$$\mathcal{L}_{\text{Presence}} = -\hat{P} \cdot \log P^* - (1 - \hat{P}) \cdot \log(1 - P^*). \quad (4)$$

The VLN is a modified version of the Faster-RCNN [28], which proposes regions and localizes the vehicle target based on the NL query. We use a standard Region Proposal Network (RPN) with anchor sizes of 32, 64, 128, 256, 512 and anchor ratios of 0.5, 1.0 and 2.0 for generating a set of region proposals. The NL Region of Interest (RoI) Head not only predicts the regression and classification as in a standard object detection RoI head, it also measures similarities between visual features for each region proposals and the NL representation, denoted as \hat{S} . The NL similarity layers are trained with a cross entropy loss that is similar to the classification loss of the RoI loss:

$$\mathcal{L}_{\text{NL}} = \sum_{\text{all regions}} -\hat{S} \log S^* - (1 - \hat{S}) \log(1 - S^*). \quad (5)$$

where S^* is the ground truth similarity. When curating the ground truth labels for training the RPN and NL RoI Head, all vehicles in the frame are marked as positive. However,

Model		AUC Success (%)	Normalized Precision (% at 0.5)
Baseline Retrieval Model	DeepSORT [34]	Mask RCNN [9]	0.66
		YOLOv3 [27]	0.92
		SSD512 [19]	<i>2.13</i>
	MOANA [30]	Mask RCNN [9]	0.52
		YOLOv3 [27]	1.69
		SSD512 [19]	0.94
	TNT [30]	Mask RCNN [9]	1.07
		YOLOv3 [27]	0.66
		SSD512 [19]	1.56
Vehicle Tracking Network (VTN)		5.93	3.79

Table 2: AUC of Success Rate Plot and Normalized Precision on the test split of the CityFlow-NL. We compare the VTN (Fig. 9) against the baseline ”track-then-retrieve” approach (Fig. 8) that was instantiated with baseline multi-object trackers. DeepSORT [34], MOANA [30], and TNT [12] with three different sets of vehicle detections: MaskRCNN [9], YOLO3 [27], and SSD512 [19] are reported here. Best and second best entries are marked with bold and italic fonts respectively.



Figure 11: Failure case of the VTN when compared to the baseline tracking model. Blue bounding boxes are results from the VTN; red bounding boxes are results from the baseline tracking model with DeepSORT [34] and YOLOv3 [27]; green bounding boxes are the ground truth. It is worth notice that the VTN is an one pass and online tracker, which predicts the highest scored bounding box when the VPN predicts that the target is present. Thus, the false positive rate is higher than the baseline tracking model, especially when there are contrasting vehicle targets in the same video.

the target similarity $S^* = 1$ if and only if the region’s target regression ground truth bounding box is exactly what the NL description refers to.

Thus, the loss for the localization branch is:

$$\mathcal{L}_{\text{Localization}} = \mathcal{L}_{\text{RPN}} + \mathcal{L}_{\text{RoI}} + \mathcal{L}_{\text{NL}}, \quad (6)$$

where \mathcal{L}_{RPN} and \mathcal{L}_{RoI} is the same as in [28]. The two branches in the VTN are jointly trained end-to-end with the above-mentioned losses:

$$\mathcal{L}_{\text{VTN}} = \mathcal{L}_{\text{Presence}} + \mathcal{L}_{\text{Localization}}. \quad (7)$$

The VTN is initialized with pretrained weights of a Faster-RCNN with FPN trained for MSCOCO. We train the RPN and RoI Head with an initial learning rate of 0.001 and the VPN with an initial learning rate of 0.01. The learning rate is decayed by 0.5 every 2,000 steps with a batch size of 16 frames distributed across 4 GPUs using a stochastic gradient descent optimizer.

When used during inference, we use the VPN with a threshold of 0.5 that is validated on the training split to indicate if the target is present in a frame. If the target is found in the frame, the VLN is then used to predict the similarities between detected vehicle bounding boxes and the NL query. We apply a sub-window attention [6] to the similarities and pick the highest scored one as the prediction for the frame.

Results for the vehicle tracking task are presented in Tbl. 2. The VTN outperforms baseline trackers and runs at 20 fps on a single GPU. As the VTN performs the NL retrieval at an earlier step during the detection phase, the recall of the targets is improved compared to the baseline trackers, which perform the NL retrieval at the last step after multi-object tracking. A failure case of the VTN is shown in Fig. 11. As the VTN is designed as an online tracker by NL detection and predicts the highest scored bounding box when the VPN predicts that the target is present, the false positive rate is higher than the baseline tracking model, especially when contrasting vehicle targets are present.

6. Conclusion

This paper has presented CityFlow-NL, the first city-scale multi-target multi-camera tracking with NL descriptions dataset that provides precise NL descriptions for multi-view ground truth vehicle tracks. Our NL annotations can be used to benchmark tasks like vehicle tracking and retrieval by NL, motion pattern analysis with NL, and MTMC with NL descriptions. We introduce two basic benchmark tasks with multiple baseline models utilizing the proposed CityFlow-NL: The Vehicle Retrieval by NL task and The Vehicle Tracking by NL task, facilitating future research on more advanced Vision+NL tasks and systems.

References

- [1] Lisa Anne Hendricks, Oliver Wang, Eli Shechtman, Josef Sivic, Trevor Darrell, and Bryan Russell. Localizing moments in video with natural language. In *Proc. IEEE International Conf. on Computer Vision (ICCV)*, pages 5803–5812, 2017. **1, 3, 5**
- [2] Luca Bertinetto, Jack Valmadre, João F Henriques, Andrea Vedaldi, and Philip HS Torr. Fully-convolutional siamese networks for object tracking. *arXiv preprint arXiv:1606.09549*, 2016. **7**
- [3] Jacob Devlin, Ming-Wei Chang, Kenton Lee, and Kristina Toutanova. Bert: Pre-training of deep bidirectional transformers for language understanding. *arXiv preprint arXiv:1810.04805*, 2018. **5**
- [4] Heng Fan, Liting Lin, Fan Yang, Peng Chu, Ge Deng, Sijia Yu, Hexin Bai, Yong Xu, Chunyuan Liao, and Haibin Ling. LaSOT: A high-quality benchmark for large-scale single object tracking. In *Proc. IEEE Conf. on Computer Vision and Pattern Recognition (CVPR)*, pages 5374–5383, 2019. **2, 3, 4**
- [5] Qi Feng, Vitaly Ablavsky, Qinxun Bai, Guorong Li, and Stan Sclaroff. Real-time visual object tracking with natural language description. In *Proc. Winter Conf. on Applications of Computer Vision (WACV)*, pages 700–709, 2020. **1, 2, 4, 7**
- [6] Qi Feng, Vitaly Ablavsky, Qinxun Bai, and Stan Sclaroff. Robust visual object tracking with natural language region proposal network. *arXiv preprint arXiv:1912.02048*, 2019. **1, 7, 8**
- [7] Kirill Gavriluk, Amir Ghodrati, Zhenyang Li, and Cees GM Snoek. Actor and action video segmentation from a sentence. In *Proc. IEEE Conf. on Computer Vision and Pattern Recognition (CVPR)*, pages 5958–5966, 2018. **1**
- [8] Xiaoxiao Guo, Hui Wu, Yu Cheng, Steven Rennie, Gerald Tesauro, and Rogerio Feris. Dialog-based interactive image retrieval. In *Advances in Neural Information Processing Systems (NeurIPS)*, pages 678–688, 2018. **5**
- [9] Kaiming He, Georgia Gkioxari, Piotr Dollár, and Ross Girshick. Mask r-cnn. In *Proc. IEEE International Conf. on Computer Vision (ICCV)*, pages 2961–2969, 2017. **7, 8**
- [10] Kaiming He, Xiangyu Zhang, Shaoqing Ren, and Jian Sun. Identity mappings in deep residual networks. In *Proc. European Conf. on Computer Vision (ECCV)*, pages 630–645. Springer, 2016. **5**
- [11] Richang Hong, Daqing Liu, Xiaoyu Mo, Xiangnan He, and Hanwang Zhang. Learning to compose and reason with language tree structures for visual grounding. *IEEE Trans. on Pattern Analysis and Machine Intelligence (PAMI)*, 2019. **2**
- [12] Hung-Min Hsu, Tsung-Wei Huang, Gaoang Wang, Jiarui Cai, Zhichao Lei, and Jenq-Neng Hwang. Multi-camera tracking of vehicles based on deep features re-id and trajectory-based camera link models. In *Proc. IEEE Conf. on Computer Vision and Pattern Recognition (CVPR) Workshops*, pages 416–424, 2019. **7, 8**
- [13] Ronghang Hu, Marcus Rohrbach, and Trevor Darrell. Segmentation from natural language expressions. In *Proc. European Conf. on Computer Vision (ECCV)*, pages 108–124. Springer, 2016. **1**
- [14] Ronghang Hu, Huazhe Xu, Marcus Rohrbach, Jiashi Feng, Kate Saenko, and Trevor Darrell. Natural language object retrieval. In *Proc. IEEE Conf. on Computer Vision and Pattern Recognition (CVPR)*, pages 4555–4564, 2016. **5**
- [15] Justin Johnson, Andrej Karpathy, and Li Fei-Fei. Denscap: Fully convolutional localization networks for dense captioning. In *Proc. IEEE Conf. on Computer Vision and Pattern Recognition (CVPR)*, pages 4565–4574, 2016. **2, 5**
- [16] Ranjay Krishna, Yuke Zhu, Oliver Groth, Justin Johnson, Kenji Hata, Joshua Kravitz, Stephanie Chen, Yannis Kalantidis, Li-Jia Li, David A Shamma, et al. Visual genome: Connecting language and vision using crowdsourced dense image annotations. *International Journal of Computer Vision (IJCV)*, 123(1):32–73, 2017. **2**
- [17] Zhenyang Li, Ran Tao, Efstratios Gavves, Cees GM Snoek, and Arnold WM Smeulders. Tracking by natural language specification. In *Proc. IEEE Conf. on Computer Vision and Pattern Recognition (CVPR)*, pages 6495–6503, 2017. **1, 2, 3, 4, 7**
- [18] Tsung-Yi Lin, Piotr Dollár, Ross Girshick, Kaiming He, Bharath Hariharan, and Serge Belongie. Feature pyramid networks for object detection. In *Proc. IEEE Conf. on Computer Vision and Pattern Recognition (CVPR)*, pages 2117–2125, 2017. **7**
- [19] Wei Liu, Dragomir Anguelov, Dumitru Erhan, Christian Szegedy, Scott Reed, Cheng-Yang Fu, and Alexander C Berg. Ssd: Single shot multibox detector. In *Proc. European Conf. on Computer Vision (ECCV)*, pages 21–37. Springer, 2016. **7, 8**
- [20] Christopher D Manning, Hinrich Schütze, and Prabhakar Raghavan. *Introduction to information retrieval*. Cambridge University Press, 2008. **5**
- [21] Junhua Mao, Jonathan Huang, Alexander Toshev, Oana Camburu, Alan L Yuille, and Kevin Murphy. Generation and comprehension of unambiguous object descriptions. In *Proc. IEEE Conf. on Computer Vision and Pattern Recognition (CVPR)*, pages 11–20, 2016. **5**
- [22] Milind Naphade, David C Anastasiu, Anuj Sharma, Vamsi Jagrlamudi, Hyeran Jeon, Kaikai Liu, Ming-Ching Chang, Siwei Lyu, and Zeyu Gao. The nvidia ai city challenge. In *2017 IEEE SmartWorld, Ubiquitous Intelligence & Computing, Advanced & Trusted Computed, Scalable Computing & Communications, Cloud & Big Data Computing, Internet of People and Smart City Innovation (SmartWorld/SCALCOM/UIC/ATC/CBDCOM/IOP/SCI)*, pages 1–6. IEEE, 2017. **1, 4**
- [23] Milind Naphade, Ming-Ching Chang, Anuj Sharma, David C Anastasiu, Vamsi Jagarlamudi, Pranamesh Chakraborty, Tingting Huang, Shuo Wang, Ming-Yu Liu, Rama Chellappa, et al. The 2018 nvidia ai city challenge. In *Proc. IEEE Conf. on Computer Vision and Pattern Recognition (CVPR) Workshops*, pages 53–60, 2018. **1**
- [24] Milind Naphade, Zheng Tang, Ming-Ching Chang, David C Anastasiu, Anuj Sharma, Rama Chellappa, Shuo Wang, Pranamesh Chakraborty, Tingting Huang, Jenq-Neng Hwang, et al. The 2019 ai city challenge. In *Proc. IEEE Conf. on Computer Vision and Pattern Recognition (CVPR) Workshops*, pages 452–460, 2019. **1**

- [25] Milind Naphade, Shuo Wang, David C Anastasiu, Zheng Tang, Ming-Ching Chang, Xiaodong Yang, Liang Zheng, Anuj Sharma, Rama Chellappa, and Pranamesh Chakraborty. The 4th ai city challenge. In *Proc. IEEE Conf. on Computer Vision and Pattern Recognition (CVPR) Workshops*, pages 626–627, 2020. [1](#)
- [26] Bryan A Plummer, Liwei Wang, Chris M Cervantes, Juan C Caicedo, Julia Hockenmaier, and Svetlana Lazebnik. Flickr30k entities: Collecting region-to-phrase correspondences for richer image-to-sentence models. In *Proc. IEEE International Conf. on Computer Vision (ICCV)*, pages 2641–2649, 2015. [2](#)
- [27] Joseph Redmon and Ali Farhadi. Yolov3: An incremental improvement. *arXiv preprint arXiv:1804.02767*, 2018. [7](#), [8](#)
- [28] Shaoqing Ren, Kaiming He, Ross Girshick, and Jian Sun. Faster r-cnn: towards real-time object detection with region proposal networks. *IEEE Trans. on Pattern Analysis and Machine Intelligence (PAMI)*, 39(6):1137–1149, 2016. [7](#), [8](#)
- [29] Olga Russakovsky, Jia Deng, Hao Su, Jonathan Krause, Sanjeev Satheesh, Sean Ma, Zhiheng Huang, Andrej Karpathy, Aditya Khosla, Michael Bernstein, Alexander C. Berg, and Li Fei-Fei. ImageNet Large Scale Visual Recognition Challenge. *International Journal of Computer Vision (IJCV)*, 115(3):211–252, 2015. [5](#)
- [30] Zheng Tang and Jenq-Neng Hwang. Moana: An online learned adaptive appearance model for robust multiple object tracking in 3d. *IEEE Access*, 7:31934–31945, 2019. [7](#), [8](#)
- [31] Zheng Tang, Milind Naphade, Ming-Yu Liu, Xiaodong Yang, Stan Birchfield, Shuo Wang, Ratnesh Kumar, David Anastasiu, and Jenq-Neng Hwang. Cityflow: A city-scale benchmark for multi-target multi-camera vehicle tracking and re-identification. In *Proc. IEEE Conf. on Computer Vision and Pattern Recognition (CVPR)*, pages 8797–8806, 2019. [1](#), [3](#), [4](#)
- [32] Ardhendu Shekhar Tripathi, Martin Danelljan, Luc Van Gool, and Radu Timofte. Tracking the known and the unknown by leveraging semantic information. In *Proc. British Machine Vision Conference (BMVC)*, volume 2, page 6, 2019. [4](#)
- [33] Oriol Vinyals, Alexander Toshev, Samy Bengio, and Dumitru Erhan. Show and tell: A neural image caption generator. In *Proc. IEEE Conf. on Computer Vision and Pattern Recognition (CVPR)*, pages 3156–3164, 2015. [2](#), [5](#)
- [34] Nicolai Wojke, Alex Bewley, and Dietrich Paulus. Simple online and realtime tracking with a deep association metric. In *IEEE International Conference on Image Processing (ICIP)*, pages 3645–3649. IEEE, 2017. [7](#), [8](#)
- [35] Yi Wu, Jongwoo Lim, and Ming-Hsuan Yang. Online object tracking: A benchmark. In *Proc. IEEE Conf. on Computer Vision and Pattern Recognition (CVPR)*, pages 2411–2418, 2013. [6](#)
- [36] Masataka Yamaguchi, Kuniaki Saito, Yoshitaka Ushiku, and Tatsuya Harada. Spatio-temporal person retrieval via natural language queries. In *Proc. IEEE International Conf. on Computer Vision (ICCV)*, pages 1453–1462, 2017. [1](#), [3](#), [4](#)
- [37] Zhengyuan Yang, Boqing Gong, Liwei Wang, Wenbing Huang, Dong Yu, and Jiebo Luo. A fast and accurate one-stage approach to visual grounding. In *Proc. IEEE International Conf. on Computer Vision (ICCV)*, pages 4683–4693, 2019. [2](#)
- [38] Peter Young, Alice Lai, Micah Hodosh, and Julia Hockenmaier. From image descriptions to visual denotations: New similarity metrics for semantic inference over event descriptions. *Transactions of the Association for Computational Linguistics*, 2:67–78, 2014. [2](#), [5](#)
- [39] Da Zhang, Xiyang Dai, Xin Wang, Yuan-Fang Wang, and Larry S Davis. Man: Moment alignment network for natural language moment retrieval via iterative graph adjustment. In *Proc. IEEE Conf. on Computer Vision and Pattern Recognition (CVPR)*, pages 1247–1257, 2019. [1](#)